Anti-Inflammatory and Immune-Modulating Effects of Rice Callus Suspension Culture (RCSC) and Bioactive Fractions in an *in vitro* Inflammatory Bowel Disease Model

Kyle Driscoll[a], Aparna Deshpande[a], Andrew Chapp[a], Kefeng Li[b], Rupali Datta[a], Wusirika Ramakrishna[a,c*]

[a]Department of Biological Sciences, Michigan Technological University, Houghton, Michigan, USA

[b]School of Medicine, University of California, San Diego, California, USA

[c]Department of Biochemistry and Microbial Sciences, Central University of Punjab, Bathinda, Punjab, India

[*]Corresponding author: Department of Biochemistry and Microbial Sciences, Central University of Punjab, City Campus, Bathinda, Punjab 151001 India

Email: rk.wusirika@cup.edu.in; wusirika@gmail.com

ABSTRACT

Background: Rice Callus Suspension Culture (RCSC) has been shown to exhibit potent antiproliferative activity in multiple cancer cell lines. RCSC and its bioactive compounds can fill the need for drugs with no side effects.

Hypothesis/Purpose: The anti-inflammatory potential of RCSC and its bioactive fractions on normal colon epithelial cell lines, was investigated.

Study Design: Three cell lines, InEpC, NCM356 and CCD841-CoN were treated with proinflammatory cytokines followed by RCSC. Cytoplasmic and nuclear ROS were assayed with fluorescent microscopy and flow cytometer. Expression analysis of immune-related genes was performed in RCSC-treated cell lines. RCSC was fractionated using column chromatography and HPLC. Pooled fractions 10-18 was used to test for antiproliferative activity using colon adenocarcinoma cell line, SW620 and anti-inflammatory activity using CCD841-CoN. Mass spectrometric analysis was performed to identify candidate compounds in four fractions.

Results: RCSC treatment showed differential effects with higher cytoplasmic ROS levels in NCM356 and CCD841-CoN and lower ROS levels in InEpC. Nuclear generated ROS levels increased in all three treated cell lines. Flow cytometry analysis of propidium iodide stained cells indicated mitigation of cell death caused by inflammation in RCSC treated groups in both NCM356 and CCD841-CoN. Genes encoding transcription factors and cytokines were differentially regulated in NCM356 and CCD841-CoN cell lines treated with RCSC which provided insights into possible pathways. Analysis of pooled fractions 10-18 by HPLC identified 8 peaks. Cell viability assay with fractions 10-18 using SW620 showed that the number of viable cells were greatly reduced which was similar to 6X and 33X RCSC with very little effect on normal cells which similar to 1X RCSC. RCSC fractions increased nuclear and cytoplasmic ROS

versus both untreated and inflammatory control. Analysis of four fractions by mass spectrometry identified 4-deoxyphloridzin, 5'-methoxycurcumin, piceid and lupeol as candidate compounds which are likely to be responsible for the antiproliferative, anti-inflammatory and immune-regulating properties of RCSC.

Conclusion: RCSC and its fractions showed anti-inflammatory activity on inflamed colon epithelial cells. Downstream target candidate genes which are likely to mediate RCSC effects were identified. Candidate compounds responsible for the antiproliferative and anti-inflammatory activity of RCSC and its fractions provide possible drug targets.

Keywords: rice callus suspension culture; inflammation; colon; reactive oxygen species; apoptosis; bioactive fraction

Abbreviations: RCSC, rice callus suspension culture; ROS, reactive oxygen species; IBD, inflammatory bowel disease; PM, plant medium; MS, Murashige and Skoog; 2,4-D, dichlorophenoxyacetic acid; CTCF, calculated total cell fluorescence; GAPDH, glyceraldehyde 3-phosphate dehydrogenase; HPRT1, hypoxanthine phosphoribosyltransferase 1; GUSB, beta-glucuronidase; HPLC, high performance liquid chromatography; DP, decluster potential; NF-κB, nuclear factor kappa-light-chain-enhancer of activated B cells; CCL5, C-C motif ligand 5; HLA1, human leukocyte antigen 1; IKBKB, inhibitor of kappa light polypeptide gene enhancer in B-cells, kinase beta; GNLY, granulysin; CSF-2, colony-stimulating factor 2; HMOX-1, heme oxygenase decycling 1; CSF1, colony stimulating factor 1; CXCL10, C-X-C motif chemokine 10; CAMS, cell adhesion molecules; UCP2, uncoupling protein 2; MKP, MAPK phosphatase

Introduction

Plants have notoriously produced a wide variety of chemicals, which have been used for therapeutic purposes dating as far back as 1400BC to this day (Croteau et al., 2000; Thomford et al., 2018). Today, they are regarded as the single most promising factor in drug discovery due to the wide therapeutic potential of natural products with minimal side effects (Furst and Zundorf, 2014). The bioactivity of natural products comes from a unique class of compounds termed "secondary metabolites". Secondary metabolites are small in size and produced by virtually all organisms in response to biotic and abiotic stress (Ramakrishna and Ravishankar, 2011).

Plant secondary metabolites are divided into three major classes: terpenoids, alkaloids and phenylpropanoids and allied phenolic compounds. Terpenoids consist of a five-carbon precursor, isopentenyl diphosphate, which is capable of undergoing extensive structural modifications (Croteau et al., 2000; Singh and Sharma, 2015). Terpenoids are present in large amount in plants and are structurally diverse class of secondary metabolites, which are involved in a wide range of biological functions. Camphor, menthol, and pyrethrins are all examples of terpenes which act as insecticides. Alkaloids consist of one or more nitrogenous atoms and are derived mainly from L-amino acids such as tryptophan, tyrosine, phenylalanine, lysine, and arginine. Alkaloids can further be divided into true alkaloids, which are found in 20% of all plant species and contain nitrogenous atoms in heterocyclic rings, and pseudoalkaloids which are not derived from amino acids, but still contain nitrogenous atoms (Alves de Almeida et al., 2017). These metabolites have over a 3000-year history of medicinal use, from the opioid morphine, and the antiarrhythmic aimaline, to the anticholinergic atropine (Croteau et al., 2000).

Phenylpropanoids and allied phenolic compounds consist of metabolites, which are formed through the shikimate, malonate acetate pathway, and/or the phenylpropanoid and phenylpropanoid acetate pathway.

Current focus has shifted to in vitro generation of plant secondary metabolites through plant exudates. One such example is plant callus which has generated interest because of its nature of production (in vitro) compared to whole plant tissues (Cai et al., 2012). Additionally, callus generation has several benefits compared to whole plants such as large-scale generation of secondary metabolites without the need for growing plants in fields as well as ease of isolation and purification of products. Callus cultures tend to be equally effective as leaf extracts as shown in case of *A. marmelos* callus culture which was as effective in the management of diabetes as leaf extract (Arumugam et al., 2008). Callus is a mass of somatic undifferentiated totipotent cells whose suspension culture has been reported to show antiproliferative activity on multiple cancerous cell lines, with minimal effects on normal cells (Rahman et al., 2016; Deshpande et al., 2012).

Inflammatory bowel disease (IBD) has emerged as a dominant inflammatory condition affecting millions across the globe (Ananthakrishnan, 2017). Colorectal cancer, on the other hand, is the third most commonly diagnosed cancer worldwide with around 700000 deaths annually (Hadjipetrou et al., 2017). Chronic inflammation is tightly linked with carcinogenesis. Individuals diagnosed with IBD or chronic ulcerative colitis, have an increased risk of developing colorectal cancer (Kanneganti et al., 2011). Our current understanding on this transformation from a normal cell population to a neoplastic growth begins with transient exposure to biotic and abiotic stressors, which cause an immune response and release of a plethora of chemicals ranging from cytokines and chemokines to free radicals created through oxidative phosphorylation (Shacter and Weitzman, 2002; Armstrong et al., 2018). This release results in adaptive responses, stimulation

of apoptosis and angiogenesis as well as induction of pre-neoplastic mutations. While this transient response is a necessity for normal survival and function of the individual, chronic exposure leads to often-permanent neoplastic changes such as increased cell proliferation, oncogene activation, and mutagenesis (Shacter and Weitzman, 2002). These changes can eventually lead to the formation of adenomatous polyps, and ultimately malignant adenocarcinomas.

In this study, we utilized an *in vitro* IBD model, along with a colorectal adenocarcinoma cell line SW 620 to investigate the effects of RCSC and its bioactive metabolites on mitigation of inflammation. We identified and characterized active fractions in RCSC with strong ROS modulating effects. Furthermore, these fractions showed potent anticancer activity *in vitro* with minimal effects on normal cells. Putative compounds in these fractions using mass spectrometry are reported.

Materials and methods

Preparation of RCSC and plant medium

Plant Medium (PM) was made by supplementing Murashige and Skoog (MS) Medium (PhytoTechnology) with casamino acids, proline, and sucrose. The resulting mixture was dissolved in deionized water and autoclaved at 125°C for 20 min. The cooled mixture was further supplemented with Chu's N6 vitamins (PhytoTechnology) and 2,4 dichlorophenoxyacetic acid (2,4-D). Rice calli were produced from the seeds of *Oryza sativa* cultivar Nipponbare grown on solid MS medium with 2,4-D and Chu's N6 vitamins (PhytoTechnology Lab) at 28°C as described by Deshpande *et al*. (2012). The calli were incubated in the sterile liquid plant medium for three weeks. During this incubation period, compounds were secreted into the medium. RCSC

was then centrifuged at 10,000 rpm for 10 min at 4°C for purification and removal of debris followed by absorbance readings between 240 nm and 300 nm using Nanodrop. The supernatant was filter (0.2 micron) sterilized before use.

Human colon cell lines and culturing

NCM 356 was obtained and licensed for three years from INCELL (San Antonio, TX). Cells were cultured and maintained in INCELL's M300A with 10% fetal bovine serum (FBS) at 37°C with 5% CO_2 as per manufacturer's recommendation. CCD 841 CoN (ATCC® CRL-1790™) was obtained from ATCC (Manassas, VA) and cultured in Eagle's minimum essential medium (EMEM, ATCC® 30-2003) with 10% FBS at 37°C with 5% CO_2. InEpC (Clonetics™) normal human intestinal epithelial cell system was purchased from Lonza and maintained with SmGM™-2 BulletKit™ which includes supplements and growth factors, insulin, hFGF-B, hEGF, FBS and gentamicin/amphotericin-B. 800,000 viable cells of InEpC were supplied by the company. Penicillin-Streptomycin-Amphotericin B solution (ATCC® PCS-999-002) was purchased from ATCC.

Cell counting was done following the general trypan blue cell exclusion assay using a hemocytometer. Cells were initially collected from a monolayer using trypsin-EDTA, centrifuged and then re-suspended in appropriate cell culture medium. From there, 25µl of cells were added to 475µl of cell culture medium to generate a diluted 1:20 ratio of cells to medium. 50µl of the 1:20 dilution was then added to 10µl of the trypan blue stain. Finally, 10µl was utilized for cell counting on the hemocytometer. Cells were then seeded in 6, 12, 24, or 96 well plates at the required cell density and incubated for 24 hours at 37°C, 5% CO_2.

NCM 356 cell line has a heterogeneous population. The floating cells and the medium were collected and transferred to 15ml or 50ml conical tubes. The cells were then washed with calcium and magnesium free phosphate buffered saline (PBS) and kept in a separate 15ml or 50ml tube. Cells were then centrifuged at 500 x g for 5-10 minutes and re-suspended in 50-75% complete culture medium and the magnesium/calcium free PBS. Next, 2ml of trypsin-EDTA was added to the monolayer and incubated at 37°C for 5-10 minutes, followed by the addition of complete growth medium to neutralize the trypsin. Cells were then pooled for counting and seeding purposes.

Treatment with pro-inflammatory cytokine cocktail

In order to stimulate an inflammatory response *in vitro*, cells were treated with a pro-inflammatory cytokine cocktail consisting of TNF-α (100ng/ml, Sigma), IL-1β (100ng/ml, Sigma), LPS (10μg/ml, Sigma), and IFN-γ (5μg/ml, Sigma) suspended in PBS, for 0-24 hours prior to any RCSC or PM treatment.

Treatment of normal colon cell lines with RCSC and PM

When the cells reached a confluence of 70-90%, they were trypsinized and seeded in 6, 12, 24, or 96 well plates at 25,000 cells per/ml for fluorescent microscopy, and 50,000-100,000 cells/ml for flow cytometry. Following 24-hour treatment with the pro-inflammatory cytokine cocktail, the cells were treated with varying dilutions of RCSC and PM, 1:5, 1:10, 1:20, 1:40, 1:80, to determine the lowest effective dose. Four time points were used: 24, 48, 72, and 96 hours.

Fluorescent microscopy

NCM 356, CCD 841, and InEpC cells were seeded in triplicates in appropriate medium supplemented with 3% heat-inactivated FBS at 25,000 cells per milliliter. Cells were visualized using Zeiss inverted fluorescent microscope following treatment for 24 hours with pro-inflammatory cytokine cocktail and 24-96 hours with RCSC or plant medium, stains for cell viability and oxidative stress. Propidium iodide (ThermoFisher Scientific) was used to assay cell viability while CellROX® Green Reagent and CellROX® Orange Reagent were used to detect nuclear and cytoplasmic oxidative stress, respectively. Because of the limited number of cells with InEpC, only nuclear and cytoplasmic reactive oxygen species assays were performed. Cell fluorescence was quantified utilizing Image J software. Calculated total cell fluorescence (CTCF) = Integrated Density – (Area of selected cell X Mean fluorescence of background readings). Statistical significance was determined utilizing t-test, and 2-way ANOVA with Tukey's post hoc test for pairwise comparison with values represented as mean±SEM (standard error of the mean) and results were considered significant at $p<0.05$.

Flow cytometry

NCM 356 and CCD 841 CoN were seeded in 6 well Nunc™ cell culture treated dishes (Thermo Scientific), at a density $\geq 1x10^6$ cells per milliliter, for 24 hours at 37°C with 5% CO_2. Cells were then treated with an inflammatory cocktail consisting of TNF-α, IL-1β, LPS, and IFN-γ for an additional 24 hours prior to RCSC treatment. Following 24-hour inflammatory cocktail treatment, cells were treated with RCSC or PM for 48 hours at 1:40 dilution (0.5mg/ml). Following the above treatment, cells were assayed with propidium iodide to determine the effects

of inflammation, PM, and RCSC on cell death. The data was analyzed utilizing percentages above or below control levels. T-test and 2-way ANOVA with Tukey's post hoc test for pairwise comparison were utilized with values represented as mean±SEM and the results were considered to be significant at $p<0.05$.

Gene expression assay

NCM 356 and CCD 841 CoN were grown until they were 70-90% confluent. The cells were trypsinized, collected and seeded in triplicates in six-well plates at 50,000 cells/ml with 3% heat-inactivated FBS in the appropriate medium. Cells were allowed 24-hour adjustment period prior to any treatment. Cells were then treated for 24 hours with pro-inflammatory cytokine cocktail prior to 24-96 hours of RCSC or PM treatments. RNA extraction was performed using the Qiagen RNeasy® Mini Kit. Total RNA was quantified using NanoDrop spectrophotometer. An equal amount of RNA was used for cDNA synthesis using Superscript® VILO cDNA synthesis kit. TaqMan® Universal Master Mix II with UNG was used for all gene expression assays. 96-well TaqMan® Arrays for human immune response with three housekeeping genes: glyceraldehyde 3-phosphate dehydrogenase (GAPDH), hypoxanthine phosphoribosyltransferase 1 (HPRT1), and beta-glucuronidase (GUSB), were analyzed. The other 92 genes are implicated in immune function, more specifically, cell surface receptors, cell cycle and protein kinases, oxidoreductases, signal transduction, stress response, transcription factors, chemokines and cytokines along with their receptors.

Column chromatography

RCSC was separated via silica column chromatography to test and isolate active fractions. 500ml of RCSC was concentrated via rotary evaporation to 15ml to create a 33x concentrated solution. The solution was again filtered through a 0.2-micron filter and aseptically aliquoted into 50ml sterile centrifuge tubes. UV-visible spectrum was analyzed via Nanodrop. A 50ml column was packed with 10-40μm silica gel and soaked with a 20/80-methanol/chloroform solvent system. 1ml of 33x concentrated RCSC was added to the column and fractions were collected in 1ml vials.

High performance liquid chromatography (HPLC)

RCSC was fractionated using HPLC. RCSC was concentrated 33x (660mg/ml) as described above. 1ml was further centri-vaped and re-suspended in 100% methanol and/or sterile deionized water. 100μl of the sample was injected into a C18 reverse phase (Kinetex™) and/or PFP column (Kinetex™) and fractionated using a photodiode array detector (Agilent Technologies). Compounds were separated using a binary gradient of 50% methanol (solvent A) and 50% acetonitrile (solvent B) and/or 5% acetic acid (Solvent A) and 50% acetonitrile (solvent B)[1]. Total run time was 60 minutes.

Human colorectal cancer cell line SW620 culturing

The cell line selected for high throughput screening of column chromatography and HPLC fractions was SW620 obtained from ATCC. SW620 was cultured in Roswell Park Memorial Institute medium (RPMI-1640) supplemented with 10% FBS and 1% penicillin, streptomycin and amphotericin B solution (ATCC). Cells were removed from liquid nitrogen and

quickly thawed in 37°C water bath. Next, cells were immediately placed in 10ml of complete growth medium and centrifuged. 10ml of complete growth medium was added to the pellet and gently mixed and then further transferred to a sterile culture dish. Cells were incubated at 37°C, 5% CO_2, 95% humidity. Once cells reached 70-90% confluence, the medium was removed and cells were treated for 5-10 minutes with 3-4ml of trypsin-EDTA solution (Hyclone) to detach the monolayer as per manufacturer recommendations. 7ml of complete growth medium was added to the culture dish to inactivate trypsin-EDTA solution. Then, cells were collected and centrifuged at 1000rpm. The pellet was then re-suspended in complete growth medium and either passaged or seeded at the appropriate density in 6, 12, 24, or 96 well plates. Cells were subcultured at 1:2 – 1:10 ratio as per manufacturer recommendations with media renewal 2 to 3 times per week.

Cell counting was done using a hemocytometer and trypan blue cell exclusion assay. Cells were first diluted to a 1:20 ratio with cell culture medium: 25µl of cells added to 475µl of cell culture medium. 50µl of the diluted sample was then added to 10µl of the trypan blue stain. Lastly, 10µl was added to the hemocytometer for cell counting.

Cytotoxicity and anti-inflammatory assays with RCSC fractions

SW620 was initially assayed with propidium iodide ReadyProbes® reagent using fluorescent microscopy and flow cytometry following treatment with each HPLC fraction. The fractions were pooled and rotary evaporated, then resuspended in PBS and tested for bioactivity. SW620 cells were seeded in 12 well plates and grown until 70-90% confluent. Cells were treated with a 1:5 dilution of each fraction for 24-48 hours and incubated at 37°C, 5% CO2, 95% humidity. Following the incubation period, the medium was removed, cells trypsinized and then collected and re-suspended in HEPES based live cell imaging solution. Lastly, cells were treated

with propidium iodide and analyzed via flow cytometry or fluorescent microscopy. Cytotoxicity and inflammatory responses were tested in normal colon cells (CCD 841 CoN). Cells were cultured and seeded as per manufacturer recommendation. The cells were then treated for 48 hours with a 1:5 dilution of fractionated RCSC (HPLC fractions 10-18) and analyzed via flow cytometer with propidium iodide ReadyProbes®. Furthermore, reactive oxygen species (ROS) assays were utilized to analyze free radical scavenging and anti-inflammatory effects following treatment with a pro-inflammatory cytokine cocktail. Cells were treated with the pro-inflammatory cytokine cocktail for 24 hours prior to 48-hour treatment with a 1:20 dilution of RCSC fraction. Following treatments, cells were analyzed for free radical scavenging capabilities utilizing CellROX® orange cytoplasmic and green nuclear ROS probes via flow cytometer under fluorescent laser 3 and 1 (FL3 and FL1), respectively. Statistical analysis of data was performed with one-way ANOVA with Tukey's test ($p<0.05$).

Mass spectrometry analysis

Each of HPLC fraction 6, 8, 11, and 12 was resuspended in 1 ml of methanol-water (50:50) and analyzed on a SCIEX high-resolution triple TOF mass spectrometer (TripleTOF 5600, SCIEX, USA) by direct infusion. The instrument was operated on positive mode with an electrospray Turbo source. The mass scanning range for primary precursor ions (Q1 scan) was set between 100 and 1200 Da. The top three most abundant ions were then subjected to MS/MS analysis to obtain the fragments. The decluster potential (DP) was set at 90 V and the collision energy was set at 40 V. Curtain gas was 20 psi and source gas was 15 psi. Compounds were tentatively identified by searching against known MS databases including PhytoHub, ReSpect for Phytochemicals, GNPS, Metlin and mass bank. Mass tolerance was set at 0.1 Da. The purity of

the isolated compounds was >85%. The relative proportion of the four fractions was calculated based on the normalized peak area of each fraction. The internal standard used for the analysis is 4-hydroxybenzoic acid.

Results

RCSC treatment enhanced cytoplasmic ROS in NCM 356 and CCD 841 CoN, enhanced nuclear ROS in inflamed colon cell lines and reduced cytoplasmic ROS in InEpC

In order to quantitatively and qualitatively determine the effects of RCSC on three epithelial cell lines, we employed fluorescent microscopy and flow cytometry to determine free radical scavenging capabilities and propidium iodide to determine cell viability. InEpC cells treated with CellROX® orange reagent a revealed significant decrease ($p<0.05$) in cytoplasmic ROS following treatment with RCSC at 1:40 dilution for 48 hours (Fig. 1). InEpC treatment with CellROX® green nuclear ROS reagent revealed a minor increase in RCSC treated versus inflammation control (Fig. 1). In most cases, treatment with the pro-inflammatory cytokine cocktail 24 hours prior to treatment resulted in higher nuclear and cytoplasmic ROS compared to control. NCM 356 (Fig. 2) and CCD 841 CoN (Fig. 3) treatment with CellROX® green nuclear ROS probe showed a significant increase ($p<0.05$) in fluorescent intensity following treatment with RCSC at 1:40 dilution for 48 hours, while treatment with CellROX® orange cytoplasmic probe again revealed a significant increase in NCM 356 (Fig. 2, $p<0.05$), and a marginal increase in CCD 841 CoN (Fig. 3) fluorescent intensity.

NCM 356 overall morphology, as analyzed by flow cytometer, indicated an increase in cell viability and forward scatter. Both forward scatter (FSC-A) and side scatter (SSC-A) are dependent on the direction of light scattered by the cell. Forward scatter can distinguish between

cell size and shape, whereas side scatter can detect internal complexity and granularity. NCM 356 treated with CellROX® green reagent following 48hour RCSC treatment revealed significant increase in nuclear generated reactive oxygen species compared to control, inflammation, and plant medium with 4.2%, 8.2%, 30.3% of cells above baseline, versus 61.4% in RCSC treatment group under FL1 (Fig. 4, $p<0.05$). Treatment with CellROX® orange cytoplasmic ROS probe, following the same conditions as above, revealed 4.6%, 11.5%, 14% and 40.4% cells fluorescing above baseline in control, inflammation, plant medium and RCSC, respectively (Fig. 4). CCD 841 CoN treated with CellROX® green ROS displayed increase under FL1, with control, inflammation, plant medium, and RCSC treatments at 6.8%, 8.8%, 8.7% and 32.5% fluorescent intensity, respectively above the baseline (Fig. 5, $p<0.05$). Slight increase following treatment with CellROX® orange cytoplasmic ROS probe was observed by flow cytometry analysis with control at 3.9%, inflammation and plant medium at 4.6% and 6.5%, respectively, and RCSC at 9.6% of the total population under FL3 (Fig. 5).

RCSC treatment reduced the effect of inflammation on cell death in NCM 356 and CCD 841 CoN

NCM 356 treated with the pro-inflammatory cytokine cocktail for 24 hours followed by 48-hour treatment of RCSC at 1:40 dilution showed a significant increase in cell viability following staining with propidium iodide when the samples were analyzed with FL3 (Fig. 6, $p<0.05$). Control revealed 96.9% viable cells, compared with 24.9% and 16.4% in inflammatory and PM controls, respectively, followed by 54.6% viable cells in RCSC treated group. This is suggestive of RCSC reducing cytokine-induced cell death. Following the same conditions as above, for CCD 841 CoN, RCSC increased cell survivability to 89.5% versus inflammation and plant medium at 79.5% and 85.5%, respectively (Fig. 6).

Genes differentially regulated with RCSC treatment identified by quantitative real-time PCR

Gene expression profile in NCM356 and CCD 841 CoN was investigated to identify possible molecular targets utilized by RCSC to control inflammation. Two genes were upregulated two-fold and four genes were downregulated ≥two-fold in NCM 356 following treatment with the pro-inflammatory cytokine cocktail and RCSC (Table 1). The gene encoding cluster of differentiation 38 (CD38) was downregulated four-fold. Two other genes, nuclear factor kappa-light-chain- enhancer of activated B cells (NF-κB) and the oncogene, SKI were upregulated in RCSC versus inflammation and plant medium controls. Furthermore, four genes, C-C motif ligand 5 (RANTES/CCL5), human leukocyte antigen 1 (HLA1) and inhibitor of kappa light polypeptide gene enhancer in B-cells, kinase beta (IKBKB) were downregulated 2-fold whereas CD38 was downregulated 4-fold in RCSC. Four genes, interleukin 1 alpha (IL-1A), granulysin (GNLY), colony-stimulating factor 2 (CSF-2), and heme oxygenase decycling 1 (HMOX-1) were upregulated ≥4-fold in CCD 841 CoN in RCSC versus inflammatory control groups, Conversely, six genes were downregulated ≥two-fold in RCSC versus inflammatory control, with three genes being downregulated ≥4-fold include SMAD family member 3 (SMAD3), colony stimulating factor 1 (CSF1), and C-X-C motif chemokine 10 (CXCL10).

Fractionation of RCSC with column chromatography and HPLC

Column chromatography was utilized to separate compounds from the 33X concentrated RCSC solution. A total of 25 fractions (1 ml each) were collected with varying mobile phases. Fractions 1-7 were collected utilizing a 20/80 methanol/chloroform mobile phase. Fractions 8-25 were collected via a 100% methanol mobile phase. Each fraction was further analyzed by HPLC

on a C18 column with 50/50 methanol/acetonitrile mobile phase, with UV 255nm for compound identification. Fractions 1-7 yielded 6 different peaks, while fractions 8-25 yielded 3 different peaks. Similar HPLC peaks resulted in pooling of the selected fractions for testing, as they likely contained the same compounds. Fractions 10-18 were pooled and further analyzed by HPLC on a C18 column which resulted in a total of 8 peaks (Fig. S1).

RCSC fractions 10-18 and RCSC concentrates increased cell death in human colon adenocarcinoma cell line SW620 compared to unfractionated 1X RCSC

A 1:5 dilution of RCSC (1X) and concentrates (3X, 6X and 33X) and fractions 10-18 were tested for antiproliferative activity using propidium iodide staining with a fluorescent microscope and flow cytometry against the human colon adenocarcinoma cell line, SW620. Furthermore, a dose-response curve was constructed. A 1:5 dilution was utilized for testing of the fractions, as this dilution factor resulted in the greatest inhibitory effect by RCSC on SW620. Following a 30-minute treatment with fractions 10-18, a significant increase in fluorescence versus untreated control was observed with a fluorescent microscope indicating a reduction in the number of viable cells. Additionally, cells showed characteristics of apoptosis such as nuclear condensation and visual apoptotic bodies. Flow cytometry analysis showed that RCSC increased cell death to 7.7%, 3X concentrated RCSC to 18.9%, 6X RCSC to 77.1%, and 33X to 78% versus untreated control at 5% (Fig. 7). Additionally, the dose-response curve calculated using the above concentrations resulted in an EC_{50} dilution factor being 3.64(Fig. 7). The EC_{50} value represents the dilution factor of the compound in which 50% of the maximal effect is observed. In this case, 50% of the SW620 cells would die following treatment with RCSC at a 1:3.64 dilution of the

3X/6X concentrated RCSC. Data was analyzed utilizing one-way ANOVA with Tukey's test ($p<0.05$) for both fluorescent microscopy and flow cytometry (n=5).

RCSC fractions 10-18 showed less toxicity compared to RCSC on normal human colon cell line CCD 841 CoN

RCSC fractions 10-18 and its concentrates were tested for effects on cell death in the normal colon cell line CCD 841 CoN treated for 48 hours followed by propidium iodide staining and flow cytometry. Cell death increased slightly in fractions 10-18 group to 8.5%, 1X RCSC group to 9.6%, 3X group to 11.8%, 6X group to 21.4%, and 33X group to 22.1% versus 4.4% in the untreated control (Fig. 7). Furthermore, a dose-response curve was generated using the above concentrates and resulted in EC_{50} dilution factor of 4.38 (Fig. 7). These results indicate that the purification of fractions 10-18 reduced the toxicity compared to 33X concentrated RCSC.

RCSC fractions 10-18 increased nuclear and cytoplasmic ROS in normal colon cell line CCD 841 CoN

RCSC fractions 10-18 were tested for ROS scavenging capabilities following 24-hour treatment with the pro-inflammatory cytokines, TNF-α, IL-1β, IFN-γ, and LPS. Following a 48-hour treatment period, nuclear ROS increased to 8.8% compared to 4.8% in the untreated control, and 5.8% in inflammation treated control, as analyzed by flow cytometry under FL1 (Fig. 7). Cytoplasmic ROS also increased following treatment with fractions 10-18 to 7.4% versus 3.7% in untreated control group, 4.8% in inflammation treated group, as analyzed by flow cytometer under FL3.

Compounds identified in RCSC fractions employing mass spectroscopy

Fractions 6, 8, 11, and 12 were subjected to mass spectroscopy. Fraction 6 largely constituted 4-deoxyphloridzin with a chemical formula $C_{21}H_{24}O_9$ and mass of 420.12 (Fig. 8). Fraction 8 consisted of 5'-methoxycurcumin with a chemical formula $C_{44}H_{44}O_{14}$ and mass of 796.27. Fraction 11 was piceid with a chemical formula $C_{20}H_{22}O_8$ and mass of 390.13. Fraction 12 was lupeol ($C_{30}H_{50}O$) with a mass of 426.39. The relative proportions estimated for the four fractions are 26.1% for fraction 6, 46% for fraction 8, 27.6% for fraction 11 and 0.2% for fraction 12.

Discussion

Maintenance of ROS generation and elimination is a critical mechanism in maintaining cellular homeostasis (Ye et al., 2015). High oxidative stress has been shown to play a critical role in a multitude of diseases such as aging, cancer, and neurodegeneration (El-Kenawi and Ruffell, 2017; Mittal et al., 2014). ROS regulate cell survival in a dose-dependent manner with moderate levels promoting cell proliferation and survival while high levels disrupting the required homeostasis. ROS has been shown to participate in a multitude of signaling pathways responsible for both the induction and removal of the inflammatory response (Schieber et al., 2014). ROS levels regulate a multitude of proteins required for cell adhesion, such as cell adhesion molecules (CAMS), which include selectins, integrins and some members of the immunoglobulin superfamily (Mittal et al., 2014). Elevated ROS levels increased the immunity of mice lacking uncoupling protein 2 (UCP2), to bacterial infections, thus indicating a beneficial role of moderate increases in ROS levels (Arsenijevic et al., 2000). Additionally, mice heterozygous for

mitochondrial hydroxylase which is necessary for ubiquinone synthesis (Mclk1) have elevated mitochondrial ROS levels along with elevated innate and adaptive immune responses that aid in pathogen defenses without harming surrounding tissue (Wang et al., 2010). On the contrary, antioxidants have shown to be beneficial in NRF2-deficient mice, because of their inability to regulate ROS generation and elimination (Kong et al., 2011). Although previous research has focused on the notion of ROS being responsible for several deleterious biological effects, alternate views exist on this aspect (Liu et al., 2018). Recent evidence suggests that ROS is required for proper maintenance of immune function and positively promotes healthy tissue generation and repair (Santos et al., 2018).

In the present study, InEpC treated with RCSC showed a significant decrease in cytoplasmic ROS, while no change was observed in regards to nuclear ROS levels. The greatest reduction in ROS was observed in InEpC when compared to both CCD 841 CoN and NCM 356. Although inflamed NCM 356 cells treated with RCSC showed higher nuclear ROS at 1:40 dilution, following 48 hours incubation, their overall survival increased. Since NCM 356 inappropriately expresses gastrin and secretes functional gastrin peptides, this could be indicative of a pre-malignant state (Chao et al., 2010). Because of the possible pre-malignant state of NCM 356, this could also explain the increase in nuclear ROS. Higher levels of ROS have been correlated with an increase in nuclear damage, because of the high reactivity of the free radical. ROS also acts as a transcriptional regulator mainly through interactions with NF-κB. Treatment with RCSC revealed a two-fold increase in NF-κB expression versus all controls, possibly indicative of regulated signaling. IKBKB downregulation (two-fold) showed an inverse relationship with NF-κB expression which supports the role of IKBKB as an inhibitor of NF-κB. Further, IKBKB may have a role outside of canonical signaling which requires IKBKB degradation (Trachootham et al., 2008). Since RCSC increased nuclear and cytoplasmic ROS and

overall survivability increased, this implicates ROS acting in a positive manner by inhibiting the action of the pro-inflammatory cytokine cocktail. An important point to consider is the concentration of the cytokines (both TNF-α and IL-1β used at 100ng/ml) in the inflammatory cocktail, which is sufficient to initiate apoptosis. In RCSC treated samples, the overall number of living cells stained with NucBlue® fluorescent probe was much higher, versus both inflammation and plant medium. Since most cells appeared apoptotic or necrotic in inflammation and plant medium, cells treated with RCSC revealed a drastic increase in nuclear generated ROS with a minor increase in cytoplasmic ROS. Thus, an increase in both nuclear and cytoplasmic generated ROS by RCSC, could be the mechanism, which prevents cytokine-induced cell death. TNF-α induced inflammation has been shown to induce ROS production through NADPH dependent oxidases (Morgan et al., 2008). This along with sustained JNK activation, a direct target of TNF-α, induces necrosis across multiple cell lines. The treatment of NCM 356 with the inflammatory cocktail and RCSC increased NF-κB 2-fold, which could account for the increase in survivability since NF-κB activation prevents both apoptosis and sustained JNK activation at normal levels.

The inflammatory and plant medium control groups both showed an increase in nuclear ROS, which could be attributed to treatment with TNF-α as well. Increase in ROS production can hinder the function of MAPK phosphatase (MKP) by altering a critical cysteine residue through oxidation (Shen and Pervaiz, 2006). This impinges MKP function while rendering JNK constitutively active, thus causing cell death as seen in both inflammatory and plant medium controls. IL-2, along with other interleukin class molecules, have also been implicated in regulating the intestinal epithelium through TGF-beta dependent pathways. Therefore, normal regulation of this cytokine is critical in maintaining a healthy population. It has been shown that abnormal increase in cytokines can lead to improper immune responses resulting in inflammation (Kopitar-Jerala, 2017).

CCD 841 CoN showed a large increase in nuclear generated reactive oxygen species with a mild increase in cytoplasmic generated ROS compared to all controls. This response can be attributed to RCSC having some effect on mitochondrial NADPH oxidases. A major portion of ROS is generated in the mitochondria and is utilized for both cellular defense mechanisms, such as initiating the innate and adaptive immune response as well as cell signaling (Morgan and Liu, 2011). Concerning anti-inflammatory effects, the pro-inflammatory cytokine, interferon, stimulated interferon gamma-induced protein 10 (CXCL10) 8-fold in both inflammatory and PM controls of CCD 841 CoN, whereas RCSC was able to reduce the expression back to control levels. This is a direct response related to the interactions of the pro-inflammatory cytokine cocktail (Rotondi et al., 2018). Furthermore, this chemokine activates the signal transduction pathway involving the constitutively expressed Janus family kinases, Jak, Tyk2, and Stat1, 2, 3 and 5 (Fenwick et al., 2015). Activation of this pathway has shown to be highly upregulated in inflammatory bowel disease.

The pro-inflammatory cytokine TNF-α has been extensively studied in IBD, and shown to be highly upregulated, with its concentration dependent on disease progression (Nourian et al., 2017). Almost all known members of the TNF family form trimers that interact in a multitude of ways, from initiating a strong inflammatory response to initiating cell death. Most notably, strong interactions of TNF family with FAS work to induce cell death, as well as to initiate strong immune modulatory effects (Strasser et al., 2009). In both inflammatory and PM groups, FAS was upregulated two-fold, whereas RCSC was able to mitigate this response. This could be one of the mechanisms in preventing cytokine-induced cell death. Interestingly, IL-6 was upregulated in RCSC treated groups in CCD 841 CoN. It binds to form an active IL-6sIL-6R complex, which in turn activates STAT3 (Francescone et al., 2015). This response results in colitis, as well as

triggering oncogenic event. However, IL-6 alone can prevent apoptosis, which could partially account for increased survivability in RCSC treated groups.

There is evidence for the use of small molecules, which can selectively target and disable the antioxidant pathways utilized in cancer cells (Zou et al., 2016). OA combination of one or more compounds isolated and identified through HPLC and mass spectroscopy, may be responsible for anti-inflammatory and anti-cancer effects. 4-deoxyphloridzin identified in fraction 6 is a derivative of phloridzin which is a phenolic compound found in apples and various parts of apple trees and accounts for roughly 11-36% of their total phenolic content (Boyer and Liu, 2014). They belong to a special class of phloretin 2'-glucosides which have long been known to be specific inhibitors of sodium-dependent glucose transporters, commonly known as SGLT, which have antidiuretic and antioxidant properties (Roder et al., 2014). 5'-methoxycurcumin found in fraction 8 is derived from curcumin which is the major bioactive constituent of the Indian spice turmeric and comes from the family of compounds known as curcuminoids, which have potent anti-inflammatory, antioxidant, antiviral, antifungal, and anticancer activity (Alam et al., 2018; Vahid et al., 2018). In relation to IBD, curcumin holds great promise in reducing the effects of several pro-inflammatory cytokines such as the master regulator NF-κB, TNF-α, various interleukins and other chemokines (Alam et al., 2018). In mice treated with trinitrobenzene sulphonic acid, a common model for IBD, curcumin greatly reduced diarrhea and disruption of colonic architecture. In addition, a significant reduction in myeloperoxidase and lipid peroxidation activity was observed in the inflamed intestinal mucosa. Piceid (resveratrol-3-O-β-D-glucoside) identified in fraction 11 is the glycosylated form of resveratrol, which is found abundantly in grapes and red wine at concentrations roughly three times that of the unconjugated aglycone, resveratrol (Basholli-Salihu et al., 2016). Resveratrol and its glycosylated forms are known to exert several pharmacological effects including anti-inflammatory and anticancer

effects in several biological systems both *in vivo* and *in vitro* (Nunes et al., 2017). For example, resveratrol inhibits COX-2 mRNA production in resveratrol-treated colorectal cancer cell line (Gong et al., 2017). Resveratrol strongly inhibits cell proliferation and elevates apoptosis in various cancer cell lines by arresting cell cycle at G2 phase and upregulating p53 (Li et al., 2018). Lupeol in fraction 12 is a pentacyclic triterpene commonly found in various fruits and vegetables such as mango, olive, green peppers, and gingseng oil (Beveridge et al., 2002). Several studies have reported lupeol to exhibit strong anti-inflammatory and anticancer activity. Lupeol has been shown to target a multitude of signaling pathways related to inflammation and carcinogenesis such as NF-κB, Fas, Kras, Wnt/β-catenin, phosphatidylinositol-3-kinase/Akt pathway (Saleem et al., 2009). Lupeol strongly inhibited LPS induced NF-κB signaling in intestinal epithelial cells and macrophages as well as VEGF signaling and TNF-α in human umbilical vein endothelial cells (Kangsamaksin et al., 2017; Lee et al., 2016). Lupeol also affected tumor angiogenesis and inhibited the progression of cholangiocarcinoma tumor xenografts. Most of the compounds in RCSC are potent free radical scavenging compounds. In the primary cell line InEpC, a reduction in both nuclear and cytoplasmic ROS can be probably attributed to resveratrol, the curcumin derivative and phloridzin derivative. On the other hand, both CCD 841 CoN and NCM 356 showed a large increase in both nuclear and cytoplasmic ROS, which is most likely attributed to the effects of lupeol. The increase in cell viability in all cell lines is likely due to the synergistic protective effects of all the compounds either through nuclear or mitochondrial signaling, or through denaturing of proteins through free radical generation. In either case, these effects prove to be beneficial *in-vitro*. Any one of these compounds could be responsible for one or all of the pleiotropic effects of RCSC (anti-cancer and anti-inflammatory). Although the relative proportion of fraction 8 (5'-methoxycurcumin) was the highest and fraction 12 (lupeol) was the lowest, the biological activity of RCSC may not directly correlate with the abundance of the compounds. Our study outlines ways of generating several compounds with potent biological effects outside of

growing whole plant tissues. Furthermore, the benefits of utilizing RCSC versus whole tissue include accelerated growth rate and generation of large quantities of compounds (alkaloids, terpenes, phenylpropanoids and allied phenolics). Although we were able to identify some known compounds in RCSC, several unknown compounds may be present which could account for the observed effects. Identifying these compounds could further provide new compounds to aid in treatments of inflammatory disorders like inflammatory bowel disease.

Conclusions

RCSC exhibited anti-inflammatory effects following high doses of pro-inflammatory cytokines. A large increase in ROS suggested protective and immune modulating effect of RCSC. The extent to which RCSC impacts cellular function is dependent on downstream targets such as FAS, NF-κB, CXCL10, IL-2, IL-6, as well as others needed to maintain cellular homeostasis. CXCL10 and CSF-1 were downregulated several-fold compared to both inflammation and PM controls, indicating the mode of RCSC action. RCSC fractions 10-18 showed similar responses as the whole RCSC on both colon adenocarcinoma cell line SW620 and the normal colon cell line CCD 841 CoN indicating the possibility of one or more of the compounds corresponding to eight peaks being responsible for the observed effects. The responses observed in our study of increased ROS levels as a result of treatment with RCSC fractions 10-18 containing the bioactive compound or compounds responsible suggest antiproliferative and anti-inflammatory activity. The next step would be to isolate individual compounds and test for efficacy, which could provide a new anticancer and anti-inflammatory compound with future clinical applications.

Acknowledgements

This work was supported by the National Institute of Food and Agriculture, U.S. Department of Agriculture, under award number 2014-67018-21767.

Conflict of interest

The authors do not have any conflicts of interest associated with this publication.

References

Alam MN, Almoyad M, Huq F. 2018. Polyphenols in colorectal cancer: Current state of knowledge including clinical trials and molecular mechanism of action. Biomed. Res. Int. 2018, 4154185.

Alves de Almeida AC, de-Faria FM, Dunder RJ, Manzo LP, Souza-Brito AR, Luiz-Ferreira A. 2017. Evid. Based Complement. Recent trends in pharmacological activity of alkaloids in animal colitis: Potential use for inflammatory bowel disease. Alternat. Med. 2017, 8528210.

Ananthakrishnan AN. 2017. Inflammatory Bowel Disease: Diagnosis and Therapeutics. Ed. Russell D. Cohen, Springer International Publishing, 1-11.

Arsenijevic D, Onuma H, Pecqueur C, Raimbault S, Manning BS, Miroux B, Couplan E, Alves-Guerra MC, Goubern M, Surwit R, Bouillaud F, Richard D, Collins S, Ricquier D. 2000. Disruption of the uncoupling protein-2 gene in mice reveals a role in immunity and reactive oxygen species production. Nat. Genet. 26, 435-9.

Armstrong H, Bording-Jorgensen M, Dijk S, Wine E. 2018. The complex interplay between chronic inflammation, the microbiome, and cancer: Understanding disease progression and what we can do to prevent it. Cancers 10, E83.

Arumugam, S, Kavimani, S, Kadalmani, B, Ahmed, ABA, Akbarsha, MA, Rao, MV. 2015. Antidiabetic activity of leaf and callus extracts of *Aegle marmelos* in rabbit. ScienceAsia 34, 317-321.

Basholli-Salihu, M, Schuster R, Mulla D, Praznik W, Viernstein H, Mueller M. 2016. Bioconversion of piceid to resveratrol by selected probiotic cell extracts. Bioprocess Biosyst. Eng. 39, 1879-1885.

Beveridge, THJ, Li, TSC, Drover, JCG. 2002. Phytosterol content in American ginseng seed oil. J. Agri. Food Chem. 50, 744-750.

Boyer, J., Liu, R. H. 2004. Apple phytochemicals and their health benefits. Nutr. J. 3, 5.

Cai, Z, Kastell, A, Knorr, D, Smetanska, I. 2012. Exudation: an expanding technique for continuous production and release of secondary metabolites from plant cell suspension and hairy root cultures. Plant Cell Rep. 31, 461-477.

Chao, C, Han, X, Ives, K, Park, J, Kolokoltsov, AA, Davey, RA, Moyer, MP, Hellmich, MR. 2010. CCK2 receptor expression transforms non-tumorigenic human NCM356 colonic epithelial cells into tumor forming cells. Int. J. Cancer 126, 864-875.

Croteau, R, Kutchan, TM, Lewis, NG. 2000. Natural products (secondary metabolites). Biochem. Mol. Biol. Plants 24, 1250-1319.

Deshpande, A, Dhadi, SR, Hager, EJ, Ramakrishna, W. 2012. Anticancer activity of rice callus suspension culture. Phytother. Res. 26, 1075–1081.

El-Kenawi A, Ruffell B. Inflammation, ROS, and mutagenesis. 2017. Cancer Cell 32, 727-729.

Fenwick PS, Macedo P, Kilty IC, Barnes PJ, Donnelly LE. 2015. Effect of JAK inhibitors on release of CXCL9, CXCL10 and CXCL11 from human airway epithelial cells. PLoS One 10, e0128757.

Francescone, R, Hou, V, Grivennikov, SI. 2015. Cytokines, IBD, and colitis-associated cancer. Inflamm. Bowel Dis. 21, 409-418.

Furst, R, Zundorf, I. 2014. Plant-derived anti-inflammatory compounds: hopes and disappointments regarding the translation of preclinical knowledge into clinical progress. Mediators of Inflamm. 2014, 146832.

Gong WH, Zhao N, Zhang ZM, Zhang YX, Yan L, Li JB. 2017. The inhibitory effect of resveratrol on COX-2 expression in human colorectal cancer: a promising therapeutic strategy. Eur. Rev. Med. Pharmacol. Sci. 21, 1136-1143.

Hadjipetrou, A, Anyfantakis, D, Galanakis, CG, Kastanakis, M, Kastanakis, S. 2017. Colorectal cancer, screening and primary care: A mini literature review. World J. Gastroenterol. 23, 6049-6058.

Kanneganti M, Mino-Kenudson M, Mizoguchi E. 2011. Animal models of colitis-associated carcinogenesis. J. Biomed. Biotechnol. 2011, 342637.

Kopitar-Jerala N. 2017. The role of interferons in inflammation and inflammasome activation. Front Immunol. 8, 873.

Kong, X, Thimmulappa, R, Craciun, F, Harvey, C, Singh, A, Kombairaju, P, Reddy, S. P, Remick, D, Biswal S. 2011. Am. J. Respir. Crit. Care Med. 184, 928-938.

Kangsamaksin T, Chaithongyot S, Wootthichairangsan C, Hanchaina R, Tangshewinsirikul C, Svasti J. 2017. Lupeol and stigmasterol suppress tumor angiogenesis and inhibit cholangiocarcinoma growth in mice via downregulation of tumor necrosis factor-α. PLoS ONE 12, e0189628.

Lee, C, Lee JW, Seo JY, Hwang SW, Im JP, Kim JS. 2016. Lupeol inhibits LPS-induced NF-kappa B signaling in intestinal epithelial cells and macrophages, and attenuates acute and chronic murine colitis. Life Sci. 146, 100-108.

Li L, Qiu RL, Lin Y, Cai Y, Bian Y, Fan Y, Gao XJ. 2018. Resveratrol suppresses human cervical carcinoma cell proliferation and elevates apoptosis via the mitochondrial and p53 signaling pathways. Oncol. Lett. 15, 9845-9851.

Liu, Z, Ren, Z, Zhang, J, Chuang, CC, Kandaswamy, E, Zhou, T, Zuo, L. 2018. Front. Physiol. 9, 477.

Mittal, M, Siddiqui, MR, Tran, K, Reddy, SP, Malik, AB. 2014. Reactive oxygen species in inflammation and tissue injury. Antioxid. Redox Signal. 20, 1126-1167.

Morgan, MJ, Kim, YS, Liu, ZG. 2008. TNFalpha and reactive oxygen species in necrotic cell death. Cell Res. 18, 343-349.

Morgan, MJ, Liu, ZG. 2011. Crosstalk of reactive oxygen species and NF-kB signaling. Cell Res. 21, 103-115.

Nourian M, Chaleshi V, Pishkar L, Azimzadeh P, Baradaran Ghavami S, Balaii H, Alinaghi S, Shahrokh S, Asadzadeh Aghdaei H, Zali MR. 2017. Evaluation of tumor necrosis factor (TNF)-α mRNA expression level and the rs1799964 polymorphism of the TNF-α gene in peripheral mononuclear cells of patients with inflammatory bowel diseases. Biomed. Rep. 6, 698-702.

Nunes, S., Danesi, F., Del Rio, D., Silva, P. 2017. Resveratrol and inflammatory bowel disease: the evidence so far. Nutr. Res. Rev. 31, 85-97.

Rahman, N, Dhadi, SR, Deshpande, A, Ramakrishna, W. 2016. Rice callus suspension culture inhibits growth of cell lines of multiple cancer types and induces apoptosis in lung cancer cell line. BMC Complement. Alternat. Med. 16, 427.

Ramakrishna, A, Ravishankar, GA. 2011. Influence of abiotic stress signals on secondary metabolites in plants. Plant Signal. Behav. 6, 1720-1731.

Röder PV, Geillinger KE, Zietek TS, Thorens B, Koepsell H, Daniel H. 2014. The role of SGLT1 and GLUT2 in intestinal glucose transport and sensing. PLoS ONE 9, e89977.

Rotondi M, Coperchini F, Latrofa F, Chiovato L. 2018. Role of chemokines in thyroid cancer microenvironment: Is CXCL8 the main player? Front. Endocrinol. 9, 314.

Saleem, M. 2009. Lupeol, a novel anti-inflammatory and anti-cancer dietary triterpene. Cancer Lett. 285, 109-115.

Santos, AL, Sinha, S, Lindner, AB. 2018. The good, the bad, and the ugly of ROS: New insights on aging and aging-related diseases from eukaryotic and prokaryotic model organisms.Oxid. Med. Cell Longev. 2018, 1941285.

Schieber, M, Chandel, NS. 2014. ROS function in redox signaling and oxidative stress. Current Biol. 24, R453-R462.

Shacter, E, Weitzman, SA. 2002. Chronic inflammation and cancer. Oncology 16, 217-232.

Shen, HM, Pervaiz, S. 2006. TNF receptor superfamily-induced cell death: redox-dependent execution. FASEB J. 20, 1589-1598.

Singh B, Sharma RA. 2015. Plant terpenes: defense responses, phylogenetic analysis, regulation and clinical applications. 3 Biotech 5, 129–151.

Strasser A, Jost PJ, Nagata S. 2009. The many roles of FAS receptor signaling in the immune system. Immunity 30, 180-192.

Trachootham, D, Lu, W, Ogasawara, MA, Nilsa, RD, Huang, P. 2008. Redox regulation of cell survival. Antioxid. Redox Signal. 10, 1343-1374.

Thomford NE, Senthebane DA, Rowe A, Munro D, Seele P, Maroyi A, Dzobo K. 2018. Natural products for drug discovery in the 21st century: Innovations for novel drug discovery. Int. J. Mol. Sci. 19, E1578.

Vahid, S., Amirhossein, S., Hossein, H. 2018. Turmeric (*Curcuma longa*) and its major constituent (curcumin) as nontoxic and safe substances: Review. Phytother. Res. 32, 985-995.

Wang, D., Malo, D., Hekimi, S. 2010. Elevated mitochondrial reactive oxygen species generation affects the immune response via hypoxia-inducible factor-1α in long-lived Mclk1^{+/−} mouse mutants. J. Immunol. 184, 582-590.

Ye ZW, Zhang J, Townsend DM, Tew KD. 2015. Oxidative stress, redox regulation and diseases of cellular differentiation. Biochim. Biophys. Acta 1850, 1607-21.

Zou, P. Xia, Y, Chen, T, Zhang, J, Wang, Z, Chen, W, Chen, M, Kanchana, K, Yang, S, Liang, G. 2016. Selective killing of gastric cancer cells by a small molecule targeting ROS-mediated ER stress activation. Mol. Carcinogen. 55, 1073-1086.

Table 1. Gene expression changes in cell lines treated with RCSC versus inflammatory and plant medium control

NCM 356		CCD 841 CoN	
Gene	Fold Change	Gene	Fold Change
NF-κB	↑2	CSF-2	↑8
SKI	↑2	GNLY	↑4
CCL5	↓2	IL-1A	↑4
CD38	↓4	IL-1B	↑2
HLA1	↓2	IL-6	↑2
IKBKB	↓2	IL-8	↑2
		LIF	↑2
		PTGS2	↑2
		CSF-1	↓8
		CXCL10	↓8
		FAS	↓2
		LY96	↓2
		NFATC3	↓2
		SMAD3	↓4

Figure Legends

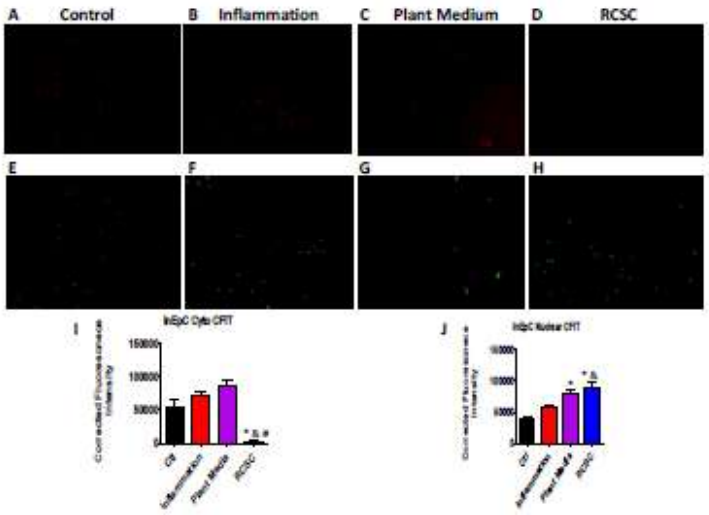

Figure 1. RCSC modulates cytoplasmic and nuclear ROS in InEpC cell line. A-D – Cytoplasmic ROS; E-H – Nuclear ROS. (A and E) Control (B and F) Inflammatory control (C and G) 1:40 Plant medium control (D and H) 1:40 RCSC (I) Quantification of cytoplasmic ROS (J) Quantification of nuclear ROS. The cell line was treated for 24 hours with inflammatory cocktail followed by treatment with 1:40 dilution of plant medium or RCSC for 48 hours followed by CellROX® orange cytoplasmic or green nuclear ROS staining. Quantification of CellROX® orange reagent and green reagent on InEpC fluorescence was performed using Image J software. All images were taken at 20x magnification using Zeiss inverted fluorescent microscope. CTCF represents Corrected Total Cell Fluorescence (n=5, $p<0.05$). Statistical analysis was performed using ANOVA with Tukey's test. * indicates significance vs. non-treated control, & indicates significance vs. inflammatory control and # indicates significance vs. plant medium control.

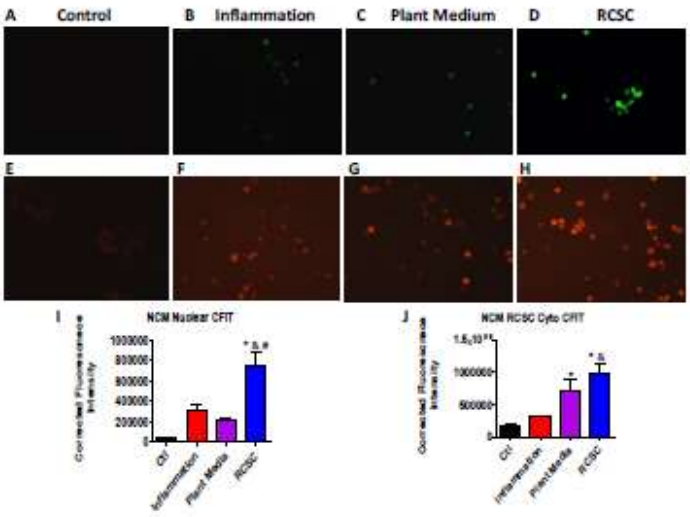

Figure 2. RCSC increases nuclear and cytoplasmic ROS in NCM 356 cell line. A-D – Nuclear ROS; E-H – Cytoplasmic ROS. (A and E) Control (B and F) Inflammatory control (C and G) 1:40 Plant medium control (D and H) 1:40 RCSC (I) Quantification of nuclear ROS (J) Quantification of cytoplasmic ROS. Treatment, analysis and quantification were as described for figure 1.

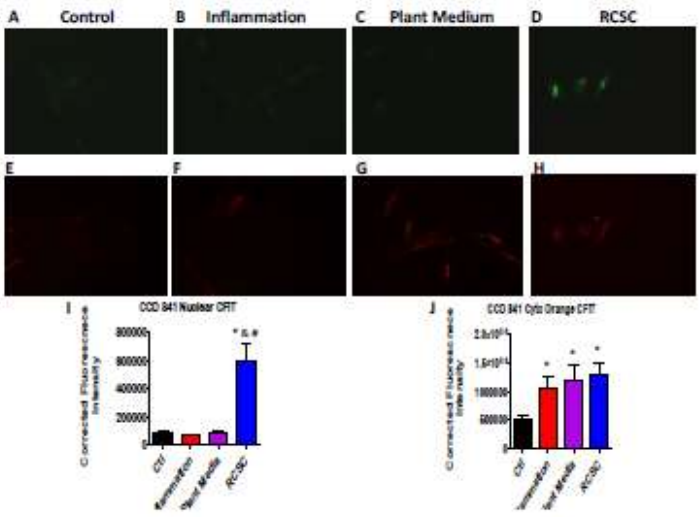

Figure 3. RCSC increases nuclear and cytoplasmic ROS in CCD 841 CoN cell line. A-D – Nuclear ROS; E-H – Cytoplasmic ROS. (A and E) Control (B and F) Inflammatory control (C and G) 1:40 Plant medium control (D and H) 1:40 RCSC (I) Quantification of nuclear ROS (J) Quantification of cytoplasmic ROS. Treatment, analysis and quantification were as described for figure 1.

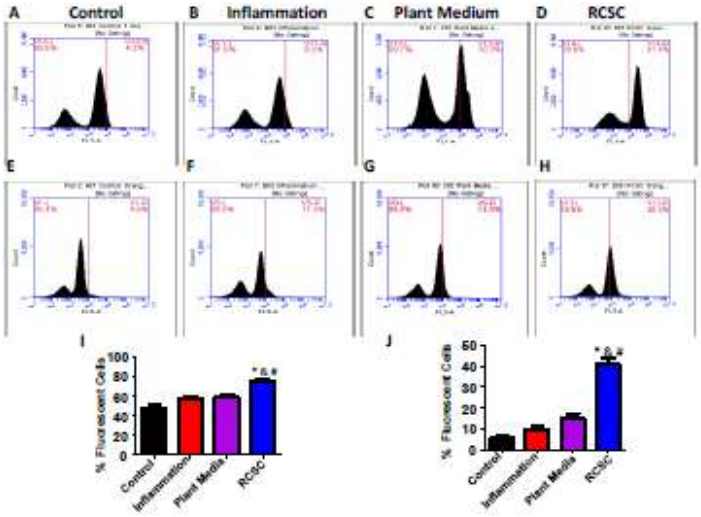

Figure 4. Flow cytometry analysis of nuclear and cytoplasmic reactive oxygen species in NCM 356 treated with RCSC. A-D – Nuclear ROS; E-H – Cytoplasmic ROS. (A and E) Control (B and F) Inflammatory control (C and G) 1:40 Plant medium control (D and H) 1:40 RCSC (I) Quantification of nuclear ROS (J) Quantification of cytoplasmic ROS. Treatment with inflammatory cocktail and RCSC was performed as described for figure 1. Cells were analyzed using BD Accuri™ C6 flow cytometer. CellROX® green nuclear stain was analyzed with fluorescent laser one (530 nm). CellROX® orange cytoplasmic stain was analyzed with fluorescent laser three (670 nm). Quantification was performed using Image J software. *= indicates significance vs. non-treated control, &= indicates significance vs.

inflammatory control, #= indicates significance vs plant medium control. Results analyzed utilizing one-way ANOVA with Tukeys test ($p<0.05$), n=100,000 cells.

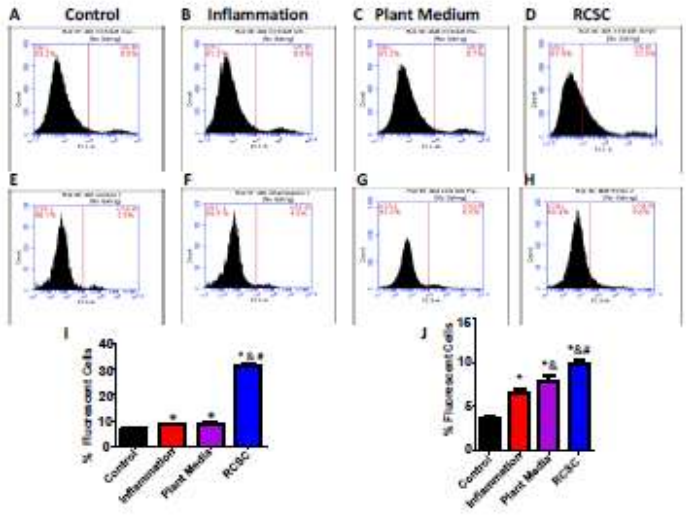

Figure 5. Flow cytometry analysis of nuclear and cytoplasmic reactive oxygen species in CCD 841 CoN treated with RCSC. A-D – Nuclear ROS; E-H – Cytoplasmic ROS. (A and E) Control (B and F) Inflammatory control (C and G) 1:40 Plant medium control (D and H) 1:40 RCSC (I) Quantification of nuclear ROS (J) Quantification of cytoplasmic ROS. Treatment, analysis and quantification were as described for figure 4.

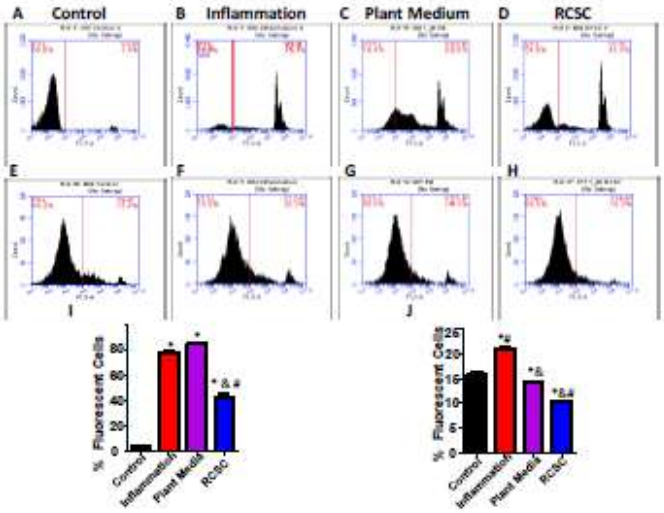

Figure 6. Flow cytometry analysis of propidium iodide in NCM 356 and CCD 841 CoN treated with rice callus suspension culture. A-D – NCM 356; E-H - CCD 841 CoN. (A) Control (B) Inflammatory control (C) 1:40 Plant medium control (D) 1:40 RCSC (E) Quantification. Cells were treated with inflammatory cocktail for 24 hours followed by 48-hour treatment with plant medium or RCSC. NCM 356 and CCD 841 CoN cell viability was assayed by propidium iodide staining followed by analysis under fluorescent laser three (FL3, 670nm filter). Statistical analysis was performed utilizing one-way ANOVA with Tukey's test, $p<0.05$.

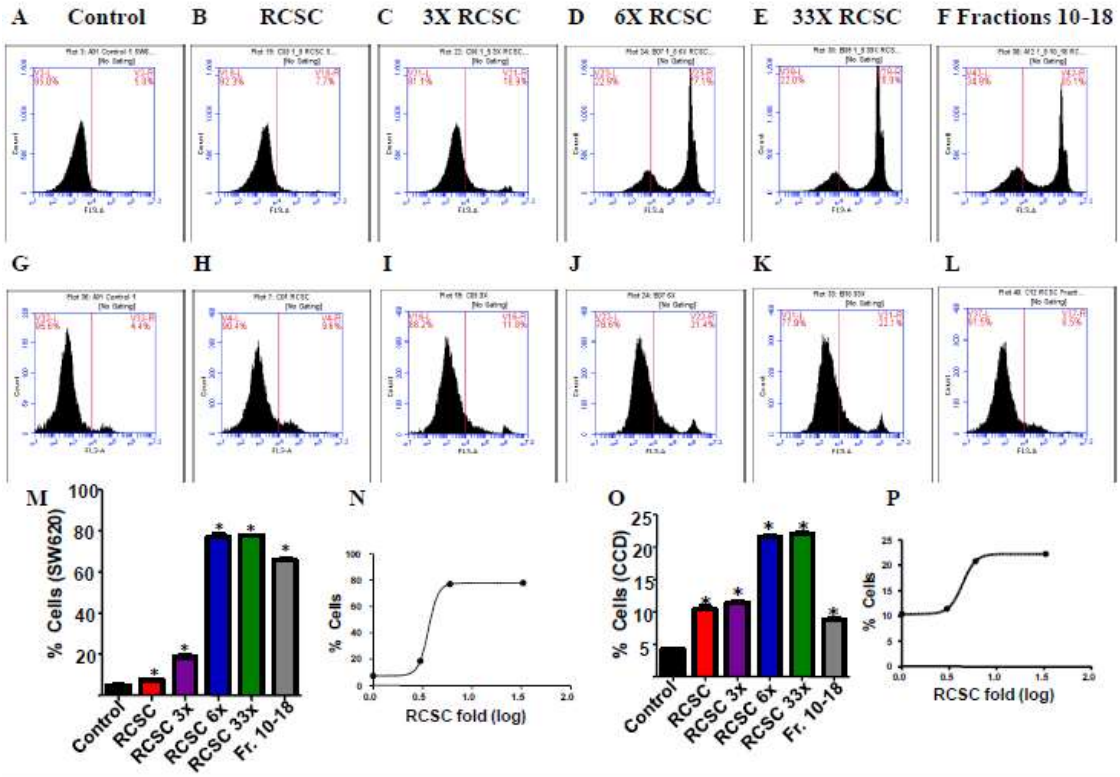

Figure 7. Flow cytometer analysis of SW620 and CCD 841 CoN treated with 1:5 dilution of RCSC, RCSC concentrates and fractions 10-18. A-F – SW620; G-L – CCD 841 CoN. (A) Control (B) RCSC (C) 3X RCSC (D) 6X RCSC (E) 33X RCSC (F) RCSC fractions 10-18 (G) Control (H) RCSC (I) 3X RCSC (J) 6X RCSC (K) 33X RCSC (L) RCSC fractions 10-18 (M) Bar graph showing quantitative data for SW620. (N) SW620 dose-response curve with varying RCSC concentrates and fractions 10-18. EC_{50}= 3.64 dilution factor. (O) Bar graph showing quantitative data for CCD 841 CoN. (P) CCD 841 CoN dose-response curve with varying RCSC concentrates and fractions 10-18. EC_{50}= 4.38 dilution factor. SW620 was treated for 30 minutes and cell viability was assayed utilizing propidium iodide staining. CCD 841 CoN was subjected to 48-hour treatment. Results were analyzed utilizing one-way ANOVA with Tukeys test, $p<0.05$. Analyzed under fluorescent laser three (FL3, 670nm filter).

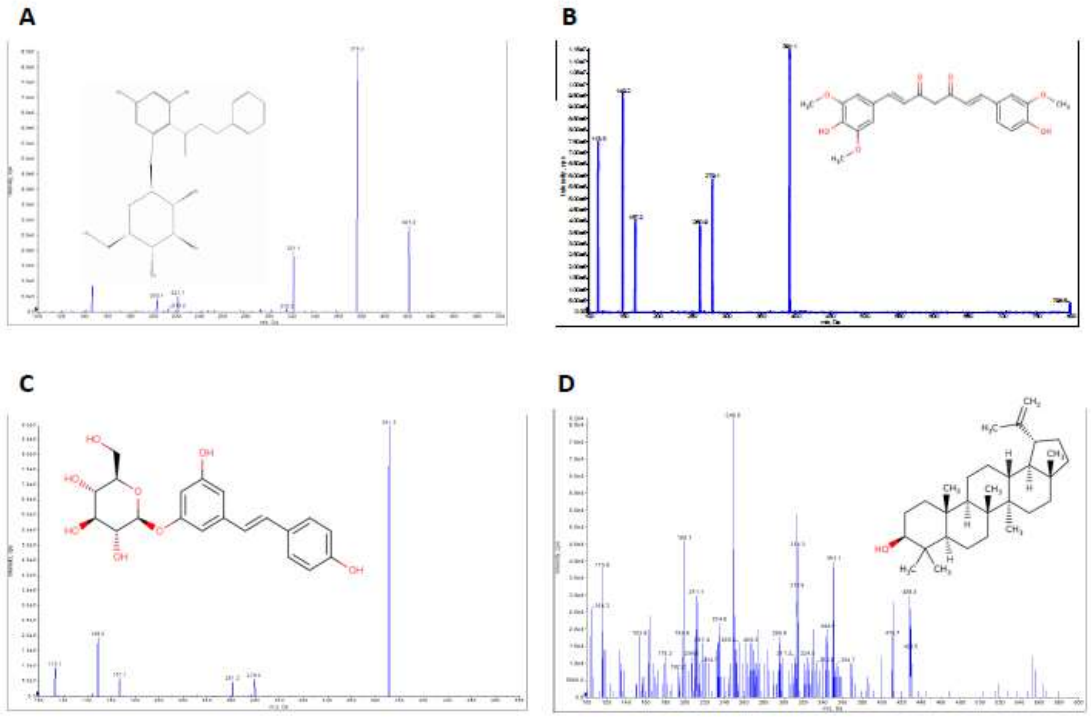

Figure 8. MS/MS fragments of candidate compounds and their structures. (A) 4-deoxyphloridzin (Fraction 6). (B) 5'-methoxycurcumin (Fraction 8). (C) Piceid (Fraction 11). (D) Lupeol (Fraction 12).

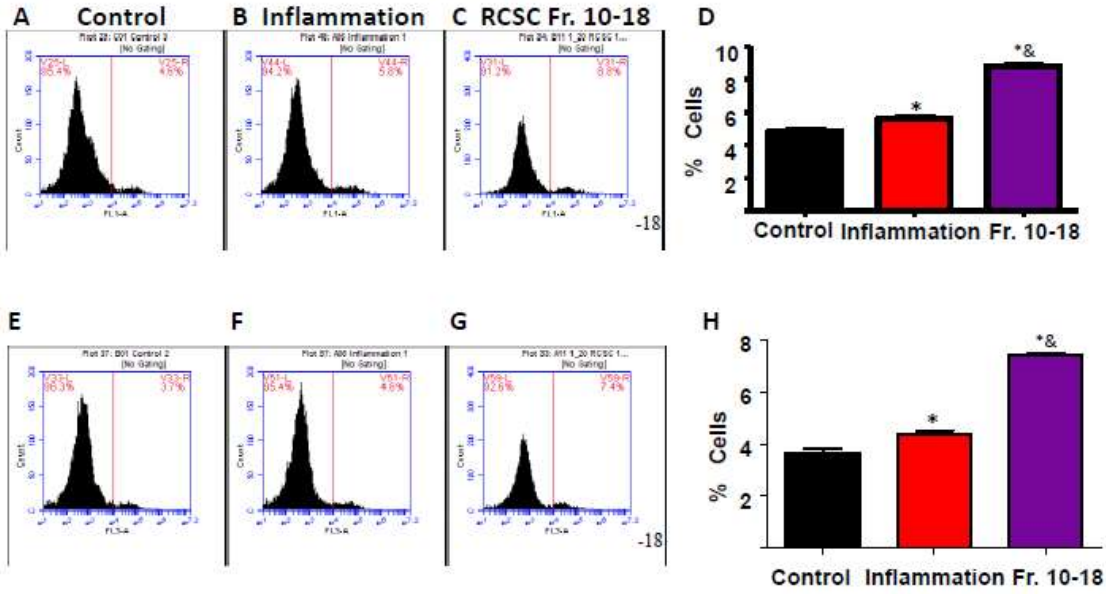

Figure 9. Flow cytometer analysis of CCD 841 CoN treated for 24 hours with inflammatory cocktail prior to 48 hours of 1:40 dilution of RCSC fractions 10-18. (A) CellROX® green nuclear stain under fluorescent laser one (530 nm). (B) Bar chart showing quantitative data. Data was analyzed utilizing one-way ANOVA with Tukeys test, $p<0.05$. (C) CellROX® orange cytoplasmic stain viewed under fluorescent laser three (670 nm). (D) Bar chart showing quantitative data. Data was analyzed utilizing one-way ANOVA with Tukeys test, $p<0.05$. n=3. Analysis was done on BD Accuri™ C6 flow cytometer.

Graphical abstract